Comparative Study on Electrical Properties of Copper Nanowire/Polypropylene and Carbon Nanotube/Polypropylene Composites

Yan Li and Uttandaraman Sundararaj
Dept. of Chemical and Petroleum Engineering, University of Calgary, Calgary, AB, Canada T2N1N4

DOI 10.1002/aic.14646
Published online October 10, 2014 in Wiley Online Library (wileyonlinelibrary.com)

Nanocomposites using copper nanowires (CuNWs) or carbon nanotubes (CNTs) as fillers with polypropylene (PP) as matrix were prepared by miscible solution mixing and precipitation method. Comparative studies on electrical conductivity and electromagnetic interference shielding properties were reported. On the conductivity curve, a plateau was found for both CuNW/PP composite and CNT/PP composite. The plateaus are located at a different concentration range for each composite type: for CuNW/PP composite, it is between 0.8 and 1.7 vol %, while for CNT/PP composite the plateau occurs in a narrower range between 0.4 and 0.6 vol %. The shielding effectiveness (SE) increases with increased concentration of fillers. CNT/PP composite has higher SE at concentrations less than 2 vol %; the two curves cross near 10 dB at this point and at concentrations higher than 2 vol %, CuNW/PP composite has higher SE. © 2014 American Institute of Chemical Engineers *AIChE J*, 61: 296–303, 2015
Keywords: conductive polymer composites, electrical properties, electromagnetic interference shielding, copper nanowire, carbon nanotube

Introduction

Conductive polymer composites (CPCs) have been intensively studied due to their many advantages, including good processability, corrosion resistance, comparatively low weight and low cost. One way to fabricate CPCs is to embed conductive fillers into a polymer matrix. Fillers include carbon black,[1,2] carbon nanotube (CNT),[3–5] carbon nanofibers,[6,7] graphene,[8,9] metal fibers,[10,11] and metal nanowires.[12,13] The composite becomes conductive once the fillers form a continuous network. The minimum loading of the conductive filler, to make the composites conductive, is known as the percolation threshold. The aspect ratio,[14] concentration and surface properties of the fillers, and the dispersion, distribution and alignment of the filler in the polymer matrix[15] will affect the percolation threshold and electrical conductivity. Studies show that by adding conductive fillers, polymer composites gain shielding property for electromagnetic interference (EMI).[16] High EMI shielding performance gives CPCs the potential to be used widely in applications such as laptops, cell phones, aircraft electronics, and medical device housings.[6] EMI is closely related to electrical conductivity. However, for certain nanocomposites with conductive fillers, studies show that even though there is a correlation between higher conductivity and higher EMI shielding effectiveness (SE), high conductivity does not necessarily lead to high EMI SE.[3,17]

Correspondence concerning this article should be addressed to U. Sundararaj at u.sundararaj@ucalgary.ca.

Highly conductive copper nanowire/polystyrene (CuNW/PS) nanocomposite, with a high EMI SE at low CuNW concentration created by miscible solution mixing and precipitation (MSMP) method[12,13] was demonstrated. A percolation threshold at 0.67 vol % CuNW was reported.[13] In this study, we are extending our studies to copper nanowire/polypropylene (CuNW/PP) composites. Several studies on PP mixed with other fillers, such as carbon black[18,19] CNT[4,20,21] can be found, but studies on CuNW as fillers are limited. The challenge is that the solution method might cause foam in the PP and this foam formation may result in difficulty in further processing. Dang et al.[22] came up with a combination of solution and melting methods which involve first solution mixing the materials, with temperature held at 100°C for solvent evaporation, followed by melting the composites at 170°C, then cooling the mixture down to room temperature to fuse the composite. In our study, we found that compression molding can be a practical method for processing PP, even if some foam is formed. Herein, we report the electrical conductivity and EMI shielding properties of the CuNW/PP composites prepared using the MSMP method.[13] As a comparison, we studied the electrical properties of the CNT/PP composites made by the same method.

Materials and Methods

CuNWs were prepared by AC electrodeposition of copper into the anodic porous aluminum oxide template.[23] The procedure includes using 25 V 8 h anodized aluminum electrodes (Alfa Aesar, 99.99+%) as templates, then using AC electrodeposition to deposit copper into the template, followed by liberation in 0.1 M sodium hydroxide solution and

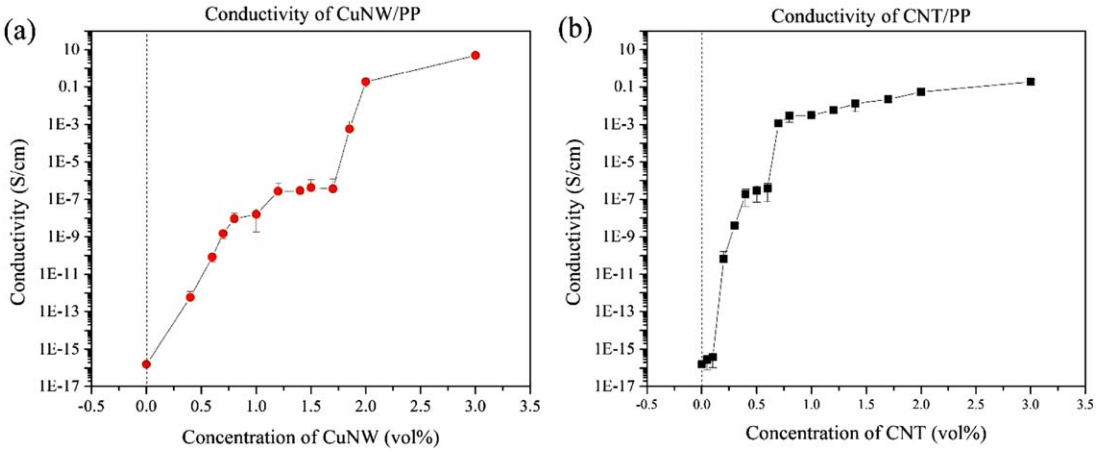

Figure 1. Volume conductivity of CuNW/PP composite (a) and CNT/PP composite (b) as a function of filler (CuNW or CNT) concentration.

[Color figure can be viewed in the online issue, which is available at wileyonlinelibrary.com.]

washing with methanol [99.8 min, British Drug Houses (BDH) Chemicals]. These CuNWs have an average diameter of 22 nm and an average length of 2.7 μm. Homopolymer PP H0500HN (Flint Hills Resources, Longview, TX) has a melt flow rate of 5g·(10 min)$^{-1}$ (ASTM D1238), a density of 0.90 g/cm^3 and a melting temperature of 165–170°C. NC7000 multiwall carbon nanotube was obtained from Nanocyl, S.A. with an average length of 1.5 μm, an average diameter of 9.5 nm, and a density of 1.73 g/cm^3.

The CuNW/PP composite powder was prepared by the MSMP method.[13] CuNWs were first dispersed in methanol, which is a nonsolvent for PP. PP was dissolved into xylene (98.5% min., BDH Chemicals) at 120°C. While the PP solution was still hot, different volumes of certain concentrations (measured by weighing CuNW) of the CuNW/methanol were dripped into the PP solution under sonication and CuNWs precipitated out with PP. Extra methanol was added until methanol–xylene ratio was 3:1 to ensure all the PP was precipitated. The mixture was filtered out and transferred into an evaporation dish which was placed in a fume hood to dry. Then, the mixture was further dried in a vacuum oven at 40°C for 2 h to remove residual solvent. The dry mixture of the CuNW/PP composite was annealed into 25 × 11.6 × 0.87 mm^3 samples by a Carver compression molder at 190°C and 34.5 MPa for 15 min. To prevent the oxidation of CuNWs, the liberation of CuNWs and the preparation of CuNW/PP composites were done in a way such that the chance of contact between CuNWs and air were minimized. There was a washing procedure with methanol which lasted less than 10 min where CuNWs had a chance for contact with air. Even here, the CuNWs were under a constant stream of methanol so oxidation was very unlikely. CNT/PP composite was prepared following the same procedure.

Transmission electron microscopy (TEM) images were taken with a Tecnai F20 field emission gun transmission electron microscope under 200 kV of accelerating voltage. CuNW/PP composite was microtomed in liquid nitrogen atmosphere. Scanning electron microscopy (SEM) images were obtained using a Philips XL 30 electron microscope. Samples were coated with gold and palladium. The electrical resistivity measurements of the CuNW/PP were conducted using two different electrometers. A Keithley 6517A electrometer was connected to an 8009 test fixture, with Keithley 6524 high resistance measurement software conforming to ASTM D991-89 standards to measure resistivity higher than 10^6 Ω cm. For resistivity lower than 10^6 Ω cm, a Loresta GP resistivity meter (MCP-T610 model, Mitsubishi Chemical Co., Japan) was connected to an ESP four-pin probe to perform the test.

The EMI and SE were carried out with an Agilent Vector Network Analyzer (Model E5071C) with an X-band frequency range (8.2–12.4 GHz). Sample size used for testing is 11.6 × 25 mm^2 rectangle with a thickness of 0.87 mm. Sample holders of 140 mm were placed between two wave guides and connected to separate ports of the analyzer. The SE was calculated using Eq. 1[1]

$$\text{EMI SE} = 10\log\ (P_I/P_T) \quad (1)$$

Here, P_I is the incident power and P_T is the transmitted power.

Differential scanning calorimetry (DSC) was conducted using a DSC Q100 from TA Instruments. The temperature calibration was done with Indium (T_m=156.6°C, ΔH_m =28.4 J/g). The analyses were done in a nitrogen atmosphere, using standard aluminum pans. Samples (4–6 mg) were heated to 250°C, with a heating rate of 10°C/min, held for 5 min to erase the thermal history effects, then cooled down to −30°C, followed by reheating to 250°C, with a heating rate of 10°C/min.

X-Ray Diffraction (XRD) patterns were obtained from a Geigerflex 2173 XRD machine from Rigaku Corporation, with a vertical goniometer and cobalt as an X-ray source. The machine also has a scintillation detector with a graphite monochromator. The test ran from 2 degrees to 65 degrees, with 2θ at 1 degree per minute, with a 0.02 degree step size.

Results and Discussion

Electrical conductivity

The electrical conductivity of the CuNW/PP composite increased by about 18 orders of magnitude compared with pure PP (10^{-16} S/cm) by adding 3 vol % CuNW, and reached 5 S/cm at a CuNW concentration of 3.0 vol % (Figure 1a). A plateau was found on the conductivity curve around 10^{-7} S/cm at CuNW concentration from 0.8 to 1.7 vol %. For the CNT/PP composite (Figure 1b), the percolation threshold is much lower; it reached conductivity of 10^{-2} S/cm at 0.8 vol % and a conductivity of 10^{-1} S/cm at

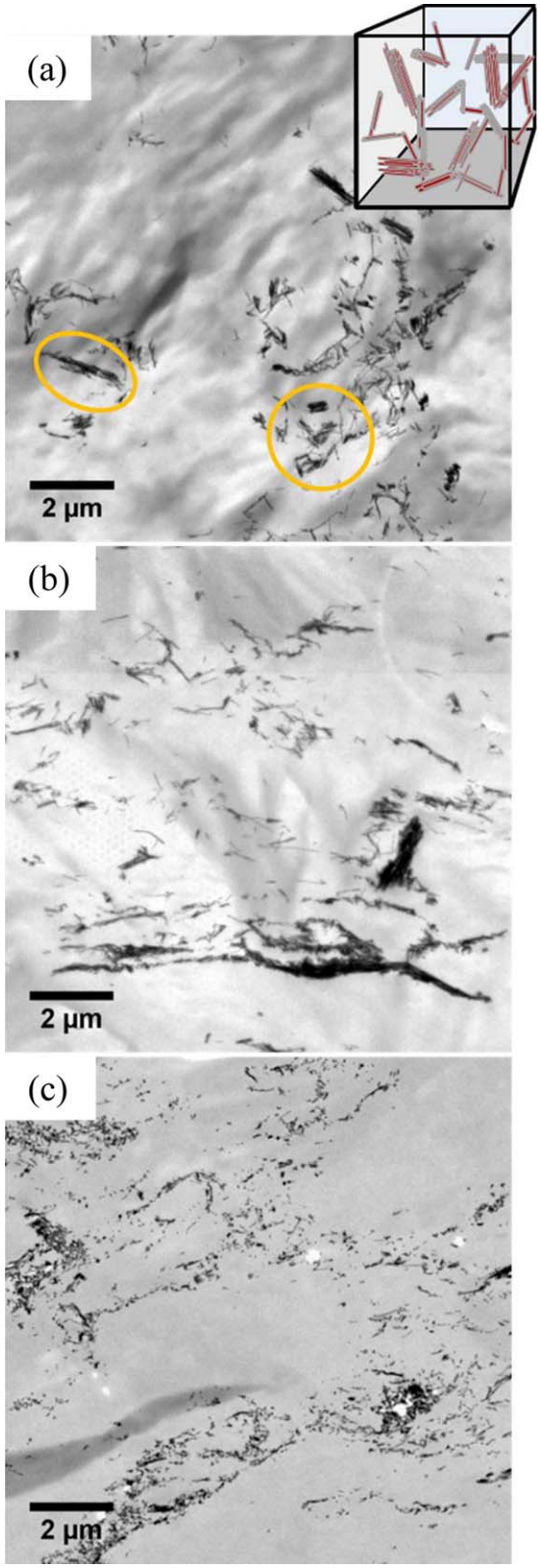

Figure 2. TEM image of cross-section of CuNW/PP composites at the concentration of 0.7 vol % (a), 1.0 vol % (b), 1.7 vol % (c), three-dimensional schematic illustration of composites is inset in (a).

[Color figure can be viewed in the online issue, which is available at wileyonlinelibrary.com.]

3.0 vol %. A narrower plateau appeared from 0.4 to 0.6 vol % of CNTs, also with conductivity of 10^{-7} S/cm. It should be noted that the conductivity of the CuNW/PP composite is much higher than the CNT/PP composite after the percolation threshold.

This is very different than the typical percolation curves reported in other studies,[13,24–27] where the conductivity increased dramatically near the percolation threshold with no plateau behavior or where a plateau was not obvious. For CuNW/PP in our study, the plateau between 0.8 and 1.7 vol % leads to a much wider percolation threshold region and it only reached high conductivity of 1 S/cm above a CuNW concentration of 1.7 vol %.

Morphology and crystallinity

To explain the plateau phenomenon, the morphology and the crystallinity of PP were studied. The MSMP method was developed to give an excellent dispersion of fillers in the matrix, which was the case when it was used with the CuNW/PS composite.[13] From the TEM image of the 0.7, 1.0, and 1.7 vol % CuNW/PP sample (Figure 2), agglomeration can be observed.

Percolation can be achieved once the conductive fillers form an effective network. However, the effective network does not necessarily mean the perfect dispersion and distribution of fillers inside the polymer matrix, since perfectly distributed fillers will have bigger gaps between the fillers.[6,28] Our hypothesis is that in PP/CuNW composites, the conductivity of the PP composites is first controlled by the distribution of the CuNW agglomeration, instead of the CuNW dispersion inside the matrix. When a certain concentration (0.7 vol %) of filler is reached, excess fillers will tend to join the clump in the formation, rather than disperse inside the polymer as a single nanowire. When the distributed clumps and dispersed fillers form an effective network, the composite becomes conductive. Network of clumps of CuNWs can be observed and some examples are shown in Figure 3.

There may be several reasons for the agglomeration of the CuNWs in the PP matrix. First, the cloud point of the PP in xylene is easily reached. The cloud point is the temperature when a phase separation occurs and the polymer starts to precipitate; it depends on the solvent/nonsolvent ratio.[29] For the CuNW/PP systems, temperature drops quickly during MSMP since the ultrasound bath temperature (80°C) is lower than the PP solution temperature (120°C). In addition, a room temperature CuNW/methanol solution is added to the PP solution and heating and evaporation of the methanol causes additional heat transfer. Once the cloud point is reached, the PP starts to precipitate out of the system. van der Waals forces between the CuNWs are strong and dominate, due to the large surface area, as compared to weak interfacial attraction between the nanowire surface and polymer chains in solution. This prevents the nanowires from being homogeneously distributed during the polymer precipitation process.

Since PP is a semicrystalline polymer, to investigate the relationship between agglomeration and composite structure, crystallinity of the composites was studied. Crystallinity of a polymer can influence the dispersion of fillers, especially when the filler has a certain tendency to distribute in either an amorphous or crystalline region.[30] DSC results were used to study the effect of adding fillers on the crystallinity of

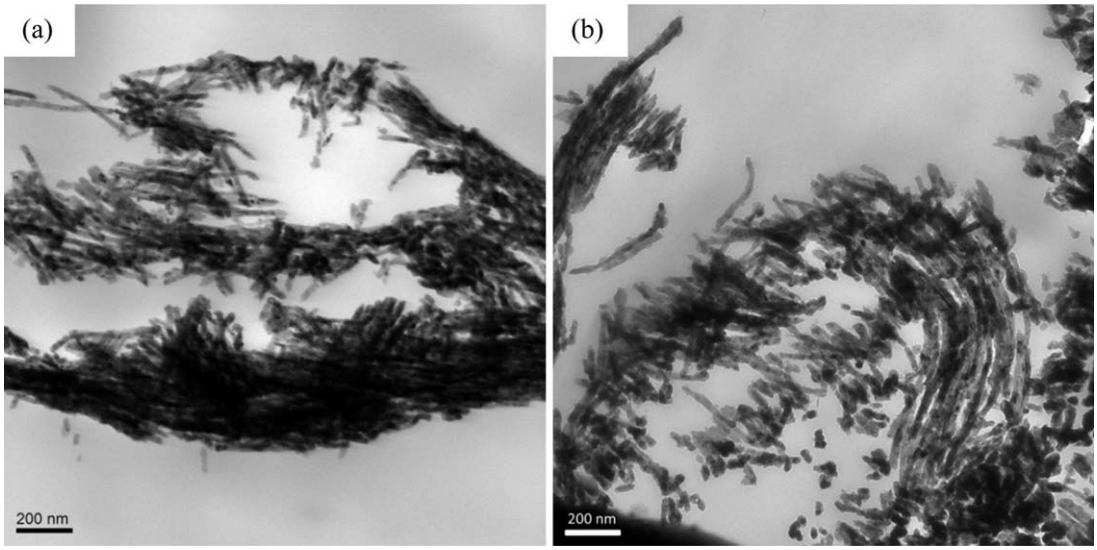

Figure 3. TEM images of CuNW/PP composite, (a) 1.0 vol %, (b) 1.7 vol %.

polymer. The information gathered from DSC includes: T_p, the peak temperature of crystallization exotherm; T_c, the temperature at the intercept of the base line and the exotherm, at the high temperature side; ΔH_c, the heat of fusion; T_m, the peak temperature of crystallization melting, and ΔH_m, the melting heat of crystallization.

T_c is the temperature where the sample starts to crystallize during the cooling process; T_p is the peak temperature of the crystallization. As shown in Figure 4a, both T_c and T_p increase with an increasing concentration of the CuNW in the composites. This means the crystallization of the sample becomes easier by adding CuNWs. Also, the increase is relatively large at the first loading of CuNWs (from 110.4°C to 118.9°C, i.e., 8.5°C difference for 0.4 vol % filler loading), compared with the higher concentration of CuNW (the difference was within 2°C when the concentration increased from 2 to 3 vol %). Based on these results, the conclusion is that the CuNWs acted as nucleating agents to accelerate the crystal growth at low loading. At higher concentrations of the CuNW, the agent becomes saturated and cannot promote the heterogeneous nucleation at the same rate. T_m is the peak temperature of crystallization melting. As shown in Figure 4b, T_m changed slightly with the different CuNW concentration, with less than 1°C difference in the whole loading range.

Crystallinity of PP can be calculated by the Eq. 2

$$X_c = \Delta H_m / \Delta H_0 \quad (2)$$

Here, ΔH_m is the melting heat of crystallization obtained from the second heating scan, ΔH_0 is the melting enthalpy of 100% crystalline PP, and $\Delta H_m = 207.1$ J/g[31,32]

For the composite, however, the crystallinity needs to be normalized to the polymer content by using Eq. 3[33]

$$X_c = \Delta H_m / \Delta H_0 (1 - W_f) \quad (3)$$

Here, W_f is the weight percentage of the filler, ΔH_m is the melting heat of crystallization, and ΔH_0 is the melting enthalpy of the 100% crystalline PP.

The crystallinity of CuNW/PP composite at different CuNW concentration is illustrated in Figure 5a. The samples show maximum crystalline fraction at CuNWs concentration of 0.4 vol %. Crystallinity then decreases with increasing CuNWs loading. This peak implies that when small amounts of the CuNWs are added to the PP matrix, the CuNWs act as nucleation agents to promote heterogeneous nucleation. The mobilization of the PP molecular chains is enhanced because adding the CuNWs accelerates the nucleation rate. However, when the loading of the CuNWs is above 2.0 vol %, the nanowires start to block the mobilization of the PP chains, resulting in a lower probability of ordered crystal lattice alignment and therefore results in decreased crystalline fraction. Surprisingly, between concentrations of 0.8–1.7 vol %, the crystallinity remains almost same. This is compelling evidence that the number of the dispersed CuNWs did not increase in the matrix, but are actually agglomerated or bundled up. When the volume fraction of the CuNWs increases, the effect of the CuNW bundles and the increasing number of dispersed nanowires result in a decreasing trend in crystallinity.

The CNT/PP composites show a peak of crystallinity of 59% at a CNT concentration of 0.1 vol % (Figure 5b). This loading is much lower than reported by Kaganj et al.[34] as they reported a peak at 1% CNT loading. One reason for the discrepancy would be the different processing technique, as Kaganj et al.[34] used melt mixing, while in this project, solution-based MSMP method is used. Similarly for the CuNW-based composite, there is a crystallinity peak on the CNT/PP curve as well. Also, crystallinity remains constant around the percolation zone (0.5 to 0.7 vol %) which is an indication of filler bundles. What is noteworthy is that the percentage drop of crystallinity from the CNT samples is not as obvious as the CuNWs samples at high concentrations (3.0 vol %). For the CNT/PP composite, all the composites have a crystalline fraction higher than that of the pure PP, and the percentage drop of crystallinity is less than 5% (59% to 55%). On the other hand, the CuNW/PP composite has a maximum crystallinity of 57% and drops to 50% at a CuNW concentration of 2 vol % and 47% at a CuNW concentration of 3 vol %.

At the same time, the introduction of fillers would affect the crystalline phase of the PP.[35–37] The PP crystalline phase can be one of four kinds: monoclinic (α), hexagonal (β), orthorhombic (γ), and mesomorphic (smectic).[35,38–41]

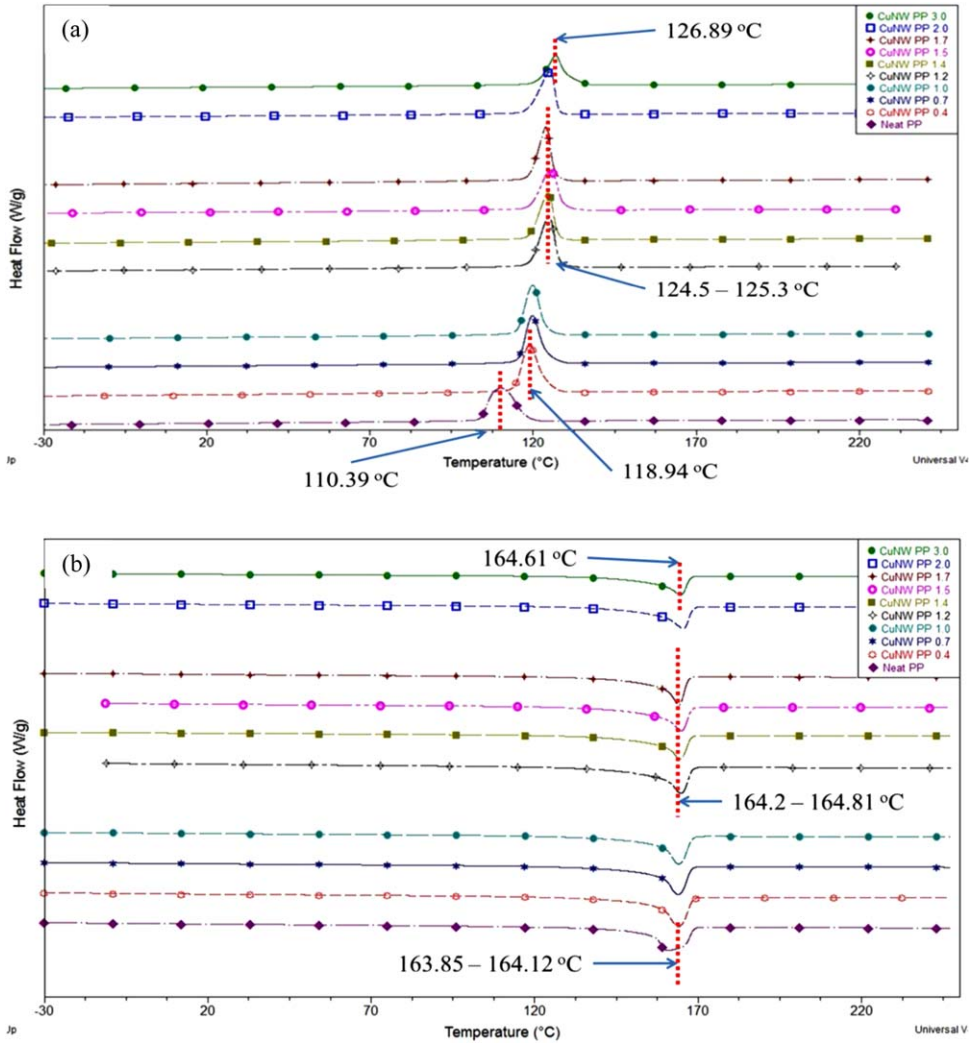

Figure 4. DSC cooling scan (a) and DSC second heating scan (b) of CuNW/PP composites at 10°C/min.

[Color figure can be viewed in the online issue, which is available at wileyonlinelibrary.com.]

Different structures result depending on the processing conditions and thermal history. Among these phases, α phase crystal is monoclinic, the most stable and most observed phase. The β phase would appear when using the β-phase nucleating agent, like carbonate[42] and silica,[43] or under specific conditions, such as temperature gradient and strain.[37,44] The crystallization of the γ phase is reported to be obtained

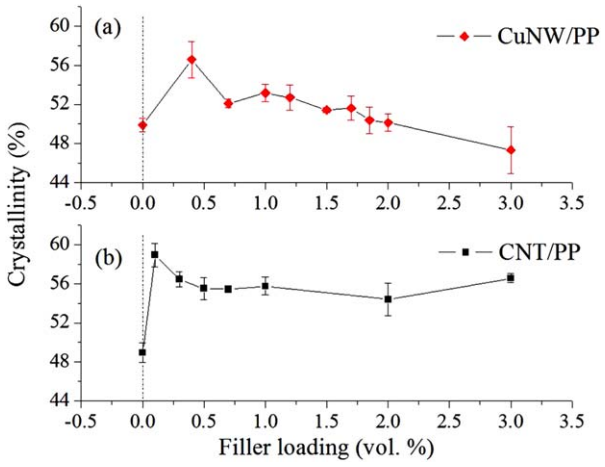

Figure 5. Crystallinity of CuNW/PP (a) and CNT/PP (b) composites. Error bar represents the standard deviation.

[Color figure can be viewed in the online issue, which is available at wileyonlinelibrary.com.]

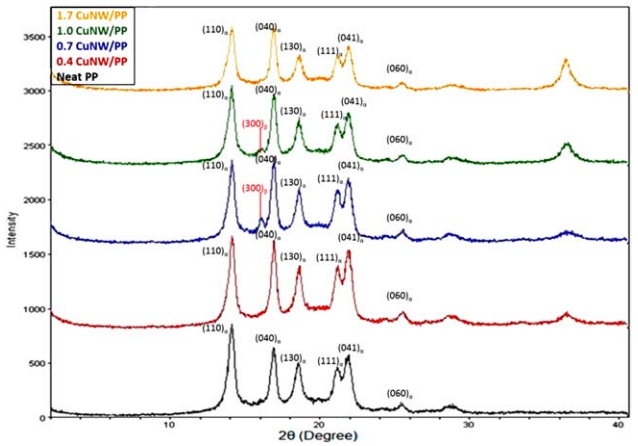

Figure 6. XRD profiles of neat PP and CuNW/PP composite with different CuNW concentrations.

[Color figure can be viewed in the online issue, which is available at wileyonlinelibrary.com.]

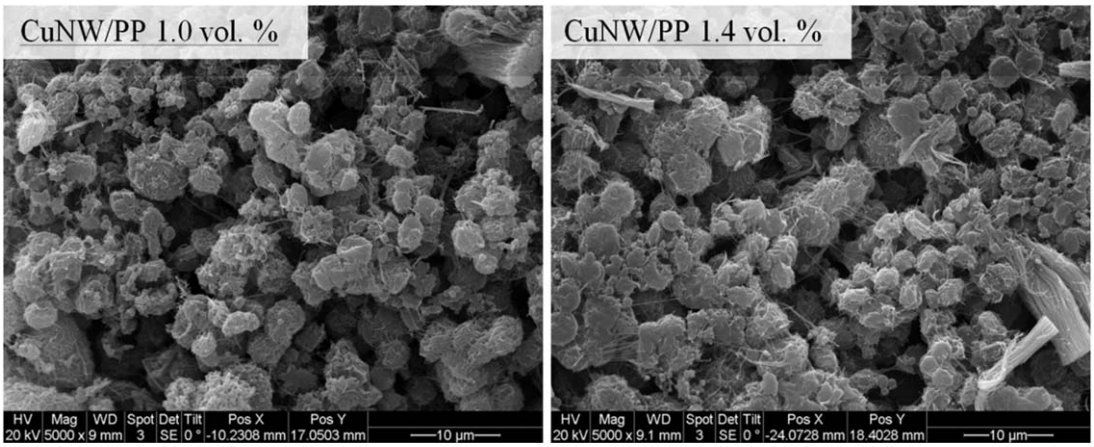

Figure 7. SEM images of CuNW/PP samples before molding with CuNW concentration 1.0 vol % (left) and 1.4 vol % (right).

under high pressure or shear flow conditions.[45,46] Not only do processing conditions affect crystal nucleation of PP but also the introduction of fillers may change the crystalline structure. Misra et al.[35] pointed out that the introduction of clay would halt the morphology of monoclinic and orthorhombic structure and promote the formation of γ phase at ambient pressure.

For the CuNW/PP composite, crystal phases can be identified by the peaks on the XRD patterns, as shown in Figure 6. Peaks can be characterized by their 2θ value. Six distinct α phase peaks are found at 2θ values of 14.2°, 17.0°, 18.7°, 21.3°, 21.7°, and 25.4°. These peaks correspond to the (110), (040), (130), (111), (041), and (060) reflections. In the composites containing 0.7 and 1.0 vol % CuNWs, the peak at 16° corresponds to the β phase (300) reflection. The γ phase crystallization peak at 20°, corresponding to the (117) reflection, is not obvious. The existence of the β phase at 16° in the CuNW/PP composites containing 0.7 and 1.0 vol % of CuNWs indicates that CuNWs can act as β-phase nucleating agents. However, the peak does not appear in the composite containing 0.4 vol % CuNW. It becomes smaller in 1.0 vol % composites as compared with 0.7 vol % and disappears entirely at higher concentrations (1.7 vol %). The assumption is that CuNWs are agglomerating at the plateau concentrations (0.7–1.7 vol %). It can be inferred that only certain sizes of agglomerations can act as β-phase nucleating agents.

The SEM images of the CuNW/PP samples before compression molding (Figure 7) show more detail about the bonding of the CuNW-PP and CuNW–CuNW. The PP forms spherical particles, by nucleation, in the solution surrounding it. The average diameter of the PP particles is 3.4 μm. CuNWs partly cover the PP particles. Some connect differently to form a network, while others bundle up to create agglomerates, with agglomerate size range from 1 to 10 μm.

EMI shielding properties

EMI SE is the ability of a material to block or reduce the intensity of the incident energy which is radiated or conducted. EMI may impair the performance of the devices. Here, EMI SE is calculated using Eq. 1 and is reported in the unit of dB.

The SE of the CuNW/PP composite is depicted in Figure 8: SE_r, SE_a, SE_o represent SE by reflection, SE by absorption and overall SE, respectively. SE_o of CuNW/PP composite is plotted over the testing frequency as shown in Figure 8a. As illustrated, SE_o increases with increasing loading of CuNW and remains constant in a small range of variation for each concentration. SE_r and SE_a are found to follow same pattern.

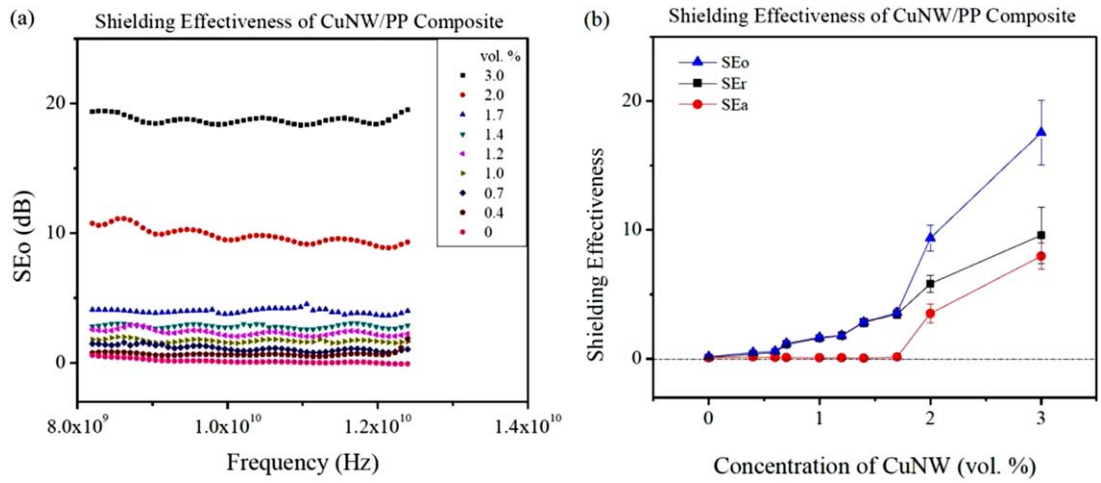

Figure 8. Overall shielding of CuNW/PP over testing frequency (a) and EMI SE of CuNW/PP composite as shown in SE by absorption, SE by reflection and overall SE (b). Error bar represents the standard deviation.

[Color figure can be viewed in the online issue, which is available at wileyonlinelibrary.com.]

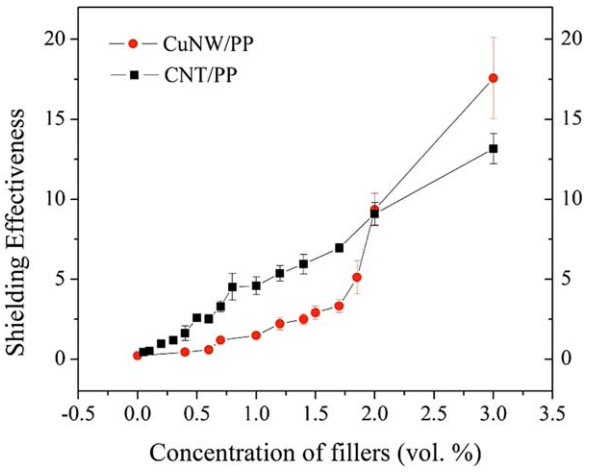

Figure 9. SE of CuNW/PP and CNT/PP composite. Error bar represents the standard deviation.

[Color figure can be viewed in the online issue, which is available at wileyonlinelibrary.com.]

Therefore, SE is obtained by averaging the value over all testing frequency, then an average SE is calculated for all samples with same concentration. In this way, SE of CuNW/PP samples with different concentrations are obtained as shown in Figure 8b. SE by reflection is caused by the mobile charge carriers. These carriers can be electrons or holes, that can interact with the electromagnetic field in the radiation.[7] Materials with higher conductivity tend to have a higher SE. SE by absorption depends on both the thickness of the shield material and the conductivity of the material. SE_a will increase when the material has electrical or magnetic dipoles which can interact with the incident power wave.

For compression molded CuNW/PP samples, the SE by reflection is dominant. The overall SE comes from the reflection of the CuNWs when the loading of the filler is lower than 1.7 vol %, while the SE by absorption remains around zero. The SE_r increases with increasing CuNW loading, demonstrating that the CuNW can interact with the electromagnetic waves regardless of whether the nanowires form a network or not. The SE_a did not increase until CuNW loading of 1.7 vol %, where the network formed.

The EMI SE is compared for the CuNW/PP and CNT/PP composites in Figure 9. For the CNT/PP composite, the formation of the conductive network started as low as 0.4 vol %. Due to this relatively low percolation threshold, the CNT/PP has a higher SE than the CuNW/PP composite when the filler volume loading is low and the conductive network in the CuNW/PP is not formed. However, after the filler loading is sufficient to form the network in the CuNW/PP composite, the EMI SE of the CuNW/PP composite is higher than the CNT/PP composite. This is because CuNWs have relatively higher conductivity and a better EMI shielding than CNT. At filler loading of 3.0 vol %, the CNT/PP composite displayed an EMI SE of 13 dB, while the EMI SE for the CuNW/PP composite was 18 dB.

Conclusions

The conductivity and EMI shielding properties of CuNW/PP and CNT/PP composites were studied and compared. The conductivity curves of both composites experience plateaus during the percolation area at different concentration ranges: for the CuNW/PP composite, it is between 0.8 and 1.7 vol % on the conductivity curve, while for the CNT/PP composite, the plateau happens between 0.4 and 0.6 vol %. Through DSC and morphology analysis, it can be concluded that the plateau is due to the agglomeration of fillers in the matrix where the extra filler joins to form bundles, therefore, no more effective networks are formed. This phenomenon is likely due to the high surface energy of the CuNW and low surface tension between the CuNW and PP matrix. The same would be true for CNT and PP matrix. The EMI shielding results were tested and compared. Both the CuNW/PP and CNT/PP composites show an increasing trend for the SE with increasing filler concentration. The CuNW/PP composite has a lower SE when the concentration of filler is below 2 vol % and higher than the CNT/PP when the loading is above 2 vol %, mainly due to the relative percolation threshold of the two fillers.

Acknowledgments

The authors acknowledge the Natural Sciences and Engineering Research Council of Canada for providing funding. The authors also thank Microscopy and Imaging Facility (MIF) of University of Calgary for providing imaging facilities.

Literature Cited

1. Das NC, Chaki TK, Khastgir D, Chakraborty A. Electromagnetic interference shielding effectiveness of conductive carbon black and carbon fiber-filled composites based on rubber and rubber blends. *Adv Polym Technol*. 2001;20(3):226–236.
2. Al-Saleh MH, Sundararaj U. An innovative method to reduce percolation threshold of carbon black filled immiscible polymer blends. *Compos Part A Appl Sci Manuf*. 2008;39(2):284–293.
3. Al-Saleh MH, Sundararaj U. Electromagnetic interference shielding mechanisms of CNT/polymer composites. *Carbon*. 2009;47(7):1738–1746.
4. Shen J, Champagne MF, Yang Z, Yu Q, Gendron R, Guo S. The development of a conductive carbon nanotube (CNT) network in CNT/polypropylene composite films during biaxial stretching. *Compos Part A Appl Sci Manuf*. 2012;43(9):1448–1453.
5. Yao X, Wu H, Wang J, Qu S, Chen G. Carbon nanotube/poly(-methyl methacrylate) (CNT/PMMA) composite electrode fabricated by in situ polymerization for microchip capillary electrophoresis. *Chemistry*. 2007;13(3):846–853.
6. Al-Saleh MH, Sundararaj U. A review of vapor grown carbon nanofiber/polymer conductive composites. *Carbon*. 2009;47(1):2–22.
7. Yang S, Lozano K, Lomeli A, Foltz HD, Jones R. Electromagnetic interference shielding effectiveness of carbon nanofiber/LCP composites. *Compos Part A Appl Sci Manuf*. 2005;36(5):691–697.
8. Stankovich S, Dikin DA, Dommett GHB, Kohlhaas KM, Zimney EJ, Stach EA, Piner RD, Nguyen ST, Ruoff RS. Graphene-based composite materials. *Nature*. 2006;442(7100):282–286.
9. Lei L, Qiu J, Sakai E. Preparing conductive poly(lactic acid) (PLA) with poly(methyl methacrylate) (PMMA) functionalized graphene (PFG) by admicellar polymerization. *Chem Eng J*. 2012;209:20–27.
10. Osawa Z, Kobayashi K. Thermal stability of shielding effectiveness of electromagnetic interference of composites. *J Mater Sci*. 1987;22(12):4381–4387.
11. Bagwell RM, McManaman JM, Wetherhold RC. Short shaped copper fibers in an epoxy matrix: their role in a multifunctional composite. *Compos Sci Technol*. 2006;66(3–4):522–530.
12. Al-Saleh MH, Gelves GA, Sundararaj U. Copper nanowire/polystyrene nanocomposites: lower percolation threshold and higher EMI shielding. *Compos Part A Appl Sci Manuf*. 2011;42(1):92–97.
13. Gelves GA, Al-Saleh MH, Sundararaj U. Highly electrically conductive and high performance EMI shielding nanowire/polymer nanocomposites by miscible mixing and precipitation. *J Mater Chem*. 2011;21(3):829.
14. Wu D, Wu L, Zhou W, Sun Y, Zhang M. Relations between the aspect ratio of carbon nanotubes and the formation of percolation

networks in biodegradable polylactide/carbon nanotube composites. *J Polym Sci Part B Polym Phys*. 2010;48(4):479–489.
15. Arjmand M, Mahmoodi M, Park S, Sundararaj U. An innovative method to reduce the energy loss of conductive filler/polymer composites for charge storage applications. *Compos Sci Technol*. 2013; 78:24–29.
16. Huang J-C. EMI shielding plastics: a review. *Adv Polym Technol*. 1995;14(2):137–150.
17. Yang Y, Gupta MC, Dudley KL, Lawrence RW. Novel carbon nanotube−polystyrene foam composites for electromagnetic interference shielding. *Nano Lett*. 2005;5(11):2131–2134.
18. Drubetski M, Siegmann A, Narkis M. Electrical properties of hybrid carbon black/carbon fiber polypropylene composites. *J Mater Sci*. 2006;42(1):1–8.
19. Al-Saleh MH, Sundararaj U. X-band EMI shielding mechanisms and shielding effectiveness of high structure carbon black/polypropylene composites. *J Phys D Appl Phys*. 2013;46(3):035304.
20. Causin V, Yang B-X, Marega C, Goh SH, Marigo A. Nucleation, structure and lamellar morphology of isotactic polypropylene filled with polypropylene-grafted multiwalled carbon nanotubes. *Eur Polym J*. 2009;45(8):2155–2163.
21. Razavi-Nouri M, Ghorbanzadeh-Ahangari M, Fereidoon A, Jahanshahi M. Effect of carbon nanotubes content on crystallization kinetics and morphology of polypropylene. *Polym Test*. 2009;28(1): 46–52.
22. Dang Y, Wang Y, Deng Y, Li M, Zhang Y, Zhang Z-W. Enhanced dielectric properties of polypropylene based composite using Bi2S3 nanorod filler. *Prog Nat Sci: Mater Int*. 2011;21(3):216–220.
23. Gelves GA, Murakami ZTM, Krantz MJ, Haber JA. Multigram synthesis of copper nanowires using ac electrodeposition into porous aluminium oxide templates. *J Mater Chem*. 2006;16(30):3075.
24. Du F, Scogna RC, Zhou W, Brand S, Fischer JE, Winey KI. Nanotube networks in polymer nanocomposites: rheology and electrical conductivity. *Macromolecules*. 2004;37(24):9048–9055.
25. Haggenmueller R, Guthy C, Lukes JR, Fischer JE, Winey KI. Single Wall Carbon nanotube/polyethylene nanocomposites: thermal and electrical conductivity. *Macromolecules*. 2007;40(7):2417–2421.
26. Moniruzzaman M, Winey KI. Polymer Nanocomposites containing carbon nanotubes. *Macromolecules*. 2006;39(16):5194–5205.
27. Ramasubramaniam R, Chen J, Liu H. Homogeneous carbon nanotube/polymer composites for electrical applications. *Appl Phys Lett*. 2003;83(14):2928–2930.
28. Gelves GA, Lin B, Haber JA, Sundararaj U. Enhancing dispersion of copper nanowires in melt-mixed polystyrene composites. *J Polym Sci Part B Polym Phys*. 2008;46(19):2064–2078.
29. Macko T, Brüll R, Pasch H. Applicability of cloud point data in liquid chromatography of polymers and continuous measurement of cloud points for polyolefins in mixed solvents. *Chromatographia*. 2003;57(1):S39–S43.
30. Gubbels F, Jerome R, Teyssie P, Vanlathem E, Deltour R, Calderone A, Parente V, Bredas JL. Selective localization of carbon black in immiscible polymer blends: a useful tool to design electrical conductive composites. *Macromolecules*. 1994;27(7):1972–1974.
31. Fatou JG. Melting temperature and enthalpy of isotactic polypropylene. *Eur Polym J*. 1971;7(8):1057–1064.
32. Cao J, Sbarski I. Determination of the enthalpy of solid phase transition for isotactic polypropylene using a modified DSC technique. *Polymer*. 2006;47(1):27–31.
33. Kessler MR. *Advanced Topics in Characterization of Composites*. Bloomington, IN: TRAFFORD Publishing, 2004.
34. Kaganj AB, Rashidi AM, Arasteh R, Taghipoor S. Crystallisation behaviour and morphological characteristics of poly(propylene)/ multi-walled carbon nanotube nanocomposites. *J Exp Nanosci*. 2009; 4(1):21–34.
35. Misra RDK, Yuan Q, Chen J, Yang Y. Hierarchical structures and phase nucleation and growth during pressure-induced crystallization of polypropylene containing dispersion of nanoclay: the impact on physical and mechanical properties. *Mater Sci Eng A*. 2010;527(9): 2163–2181.
36. Yuan Q, Deshmane C, Pesacreta TC, Misra RDK. Nanoparticle effects on spherulitic structure and phase formation in polypropylene crystallized at moderately elevated pressures: the influence on fracture resistance. *Mater Sci Eng A*. 2008;480(1–2):181–188.
37. Ginzburg VV. Influence of nanoparticles on miscibility of polymer blends. a simple theory. *Macromolecules*. 2005;38(6):2362–2367.
38. Cheng SZD, Janimak JJ, Zhang A, Hsieh ET. Isotacticity effect on crystallization and melting in polypropylene fractions: 1. Crystalline structures and thermodynamic property changes. *Polymer*. 1991; 32(4):648–655.
39. Radhakrishnan J, Ichikawa K, Yamada K, Toda A, Hikosaka M. Nearly pure $\alpha 2$ form crystals obtained by melt crystallization of high tacticity isotactic polypropylene. *Polymer*. 1998;39(13):2995–2997.
40. Varga J. Supermolecular structure of isotactic polypropylene. *J Mater Sci*. 1992;27(10):2557–2579.
41. Miller RL. On the existence of near-range order in isotactic polypropylenes. *Polymer*. 1960;1:135–143.
42. Kaplan D. *Biopolymers from Renewable Resources*. New York, USA: Springer-Verlag Berlin Heidelberg, 1998.
43. Hansen CM. *Hansen Solubility Parameters: A User's Handbook, 2nd ed*. New York, USA: Taylor & Francis, 2012.
44. Wilson JM. Gantt charts: a centenary appreciation. *Eur J Oper Res*. 2003;149(2):430–437.
45. Bhattacharya SK. *Metal Filled Polymers*. New York, USA: Taylor & Francis, 1986.
46. Blythe AR, Bloor D. Electrical Properties of Polymers. Cambridge, UK: Cambridge University Press, 2005.

Manuscript received May 9, 2014, and revision received July 23, 2014.